



**Discrimination of cellular developmental states focusing on
glycan transformation and membrane dynamics by using
BODIPY-tagged lactosyl ceramide**

Journal:	<i>Organic & Biomolecular Chemistry</i>
Manuscript ID	OB-ART-03-2020-000547.R2
Article Type:	Paper
Date Submitted by the Author:	24-Apr-2020
Complete List of Authors:	Arai, Kenta; Osaka University Ohtake, Atsuko; RIKEN, Synthetic Cellular Chemistry Laboratory Daikoku, Shusaku; RIKEN, Synthetic Cellular Chemistry Laboratory Suzuki, Katsuhiko; Aomori University Faculty of Pharmaceutical Science Ito, Yukishige; RIKEN, Synthetic Cellular Chemistry Laboratory Kabayama, Kazuya; Osaka University Fukase, Koichi; Osaka University, Graduate School of Science Kanie, Yoshimi; Tokai University, Research Promotion Division Kanie, Osamu; Tokai University, Department of Applied Biochemistry

Organic & Biomolecular Chemistry

Discrimination of cellular developmental states focusing on glycan transformation and membrane dynamics by using BODIPY-tagged lactosyl ceramide

Received 00th January 20xx,
Accepted 00th January 20xx

DOI: 10.1039/x0xx00000x

Kenta Arai,^{a†} Atsuko Ohtake,^{b†} Shusaku Daikoku,^b Katsuhiko Suzuki,^c Yukishige Ito,^{a,b}
Kazuya Kabayama,^{a,d} Koichi Fukase,^a Yoshimi Kanie,^{e†} Osamu Kanie^{*d,f}

Glycosphingolipid (GSL) is a group of molecules composed of hydrophilic glycan part and hydrophobic ceramide creating diverse family. GSLs are de novo synthesised from ceramide at endoplasmic reticulum and Golgi apparatus, and transported to outer surface of plasma membrane. It has been known that the glycan structures of GSLs changes reflecting disease states. We envisioned that analysing the glycan pattern of GSLs enables distinguishing diseases. For this purpose, we utilised a fluorescently tagged compound, LacCerBODIPY (**1**). At first, compound **1** was taken up by a cultured PC12D cells and transformed into various GSLs. As a result, change in the GSL patterns of differentiation states of the cells was successfully observed by using an analysis platform, nano liquid chromatography (LC)-fluorescence detected (FLD)-electrospray ionisation (ESI)-mass spectrometry (MS), which could quantitate and provide molecular ion simultaneously. We found that the compound **1** remained for about 10 min on the plasma membrane before it is converted into other GSLs. We therefore investigated more rapid way of discriminating different cellular states by fluorescence recovery after photobleaching, which revealed that it is possible to distinguish the differentiation states as well.

Introduction

The glycan structure distribution of glycosphingolipids (GSLs) present on the outer leaflet of the plasma membrane reflects the changes in cellular phenotypes and cellular states [1]. The glycan structures of GSLs are constructed by sequential reactions of enzymes using sugar nucleotides in the endoplasmic reticulum and Golgi apparatus. The balance of glycan synthesis and degradation rates must be kept steady in all cell types and states. Despite the accumulation of information about glycan structure reflecting the cellular states, details of the relationship between the cellular states and glycan synthesis and degradation are not well known. Various types of fluorescent tags have been utilised to investigate lipid-associated molecular basis in cellular events [2,3].

^a Department of Chemistry, Graduate School of Science, Osaka University, 1-1 Machikaneyama, Toyonaka, Osaka, 560-0043, Japan.

^b Synthetic Cellular Chemistry Laboratory, RIKEN, 2-1 Hirosawa, Wako, Satama 351-0198, Japan.

^c Faculty of Pharmaceutical Sciences, Aomori University, 2-3-1 Kohbata, Aomori 030-0943, Japan.

^d Micro/Nano Technology Center, Tokai University, 4-1-1 Kitakaname, Hiratsuka, Kanagawa, 259-1292, Japan.

^e Research promotion division, Tokai University, 4-1-1 Kitakaname, Hiratsuka, Kanagawa, 259-1292, Japan.

^f Department of Applied Biochemistry, Tokai University, 4-1-1 Kitakaname, Hiratsuka, Kanagawa, 259-1292, Japan.

† Equal contribution

Electronic Supplementary Information (ESI) available: [details of any supplementary information available should be included here]. See DOI: 10.1039/x0xx00000x

ARTICLE

OBC

Pagano *et al.* discovered that exogenous fluorescently (BODIPY-) labelled lactosyl ceramides (LacCerBODIPY) can be internalised via endocytosis and retrogradely transported to the Golgi apparatus and lysosome, where they are converted into a series of GSLs [4-7]. We are interested in intra cellular trafficking of the BODIPY-tagged molecule to further analyse its conversion process instead of analysing particular proteins interacting with the probe molecule, and selected this simple BODIPY-labelled LacCer (**1**) derivative and its analogues **2-4** (Fig. 1), and further investigated their capabilities. LacCerBODIPY **1** is useful and advantageous for investigating intracellular localisation and structure analysis using nano liquid chromatography (LC)-fluorescence detected (FLD)-electrospray ionisation (ESI)-mass spectrometry (MS) [8-11] when compared with the compound with a fluorophore attached to a carbohydrate moiety [12]. This internalisation process occurs after the recycling of endogenous GSLs. According to our previous fluorescence pulse-chasing results combined with structural analysis using MS, **1** in the form of a bovine serum albumin (BSA) complex was taken up by the cell, moved to the Golgi apparatus where multiple carbohydrates were added, and relocated to the outer surface of the cell membrane in a time-dependent manner. These events were successfully confirmed in experiments using cultured African green monkey kidney fibroblast (COS) 7 and Chinese hamster ovary (CHO)-K1 cells. We found that less than 3,000 cultured cells were sufficient for determining the structure of GSL analogues in our studies [8,9]. We observed that the fluorescence on the surface of the plasma membrane was retained for more than ten minutes after one-minute pulse introduction [9]. It was also shown that the Golgi apparatus has a limit in glycan processing where quantity of compound exceeding the capacity is delivered to lysosomes [9,10].

We hypothesised that this glycan profiling capability could be used to distinguish between undifferentiated and differentiated cellular states by tracing these phenomena. This is important because cell transformation relates to tumour malignancy and neurodegeneration. LacCerBODIPY (**1**) is an ideal candidate to distinguish whether the cells under investigation are undifferentiated or differentiated using pheochromocytoma PC12D cells, which are known to differentiate into a neuron-like state in response to neural growth factor (NGF) treatment [13-17].

Here we would like to report a series of important findings in time-resolved localisation of a fluorescent molecule derived from **1** by using fluorescence scanning confocal microscopy, time-resolved glycan processing of **1** by using nano LC-FLD-ESI-MS, and the ability of **1** to determine the three separate differentiation stages based on the fluorescence recovery after photobleaching (FRAP) that is often used to investigate membrane fluidity.

Experimental

Nomenclature of Compounds

The nomenclature of GSLs was determined in accordance with IUPAC-IUB recommendations 1977. The symbol

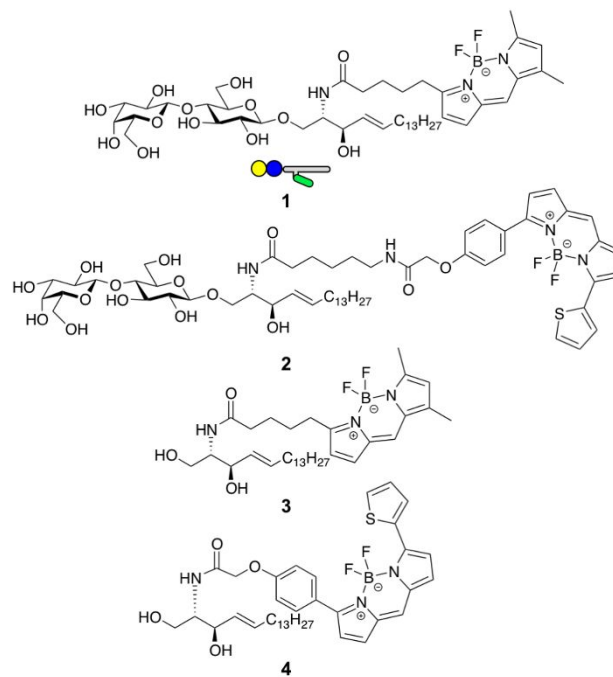


Fig. 1. Structures of the fluorescent compounds used in this study. Compound **1**: Lactosyl sphingosine carrying BODIPY C₅ (LacCerBODIPY); Compound **2**: Lactosyl sphingosine carrying BODIPY TR-X; Compound **3**: Sphingosine carrying BODIPY C₅ (CerBODIPY); Compound **4**: Sphingosine carrying BODIPY TR.

nomenclature was selected as suggested by the Consortium for Functional Glycomics. [<http://www.functionalglycomics.org/static/consortium/Nomenclature.shtml>]

General procedure

4,4-Difluoro-5,7-dimethyl-4-bora-3a,4a-diaza-s-indacene-3-pentanoic acid (BODIPY FL C₅), 6-(((4-(4,4-difluoro-5-(2-thienyl)-4-bora-3a,4a-diaza-s-indacene-3-yl)phenoxy)acetyl)amino)hexanoic acid, succinimidyl ester (BODIPY TR-X, SE), *N*-((4-(4,4-difluoro-5-(2-thienyl)-4-bora-3a,4a-diaza-s-indacene-3-yl)phenoxy)acetyl)sphingosine (Ceramide BODIPY TR; Compound **4**), and GlutaMAX-I were purchased from Thermo Fisher Scientific (MA, USA). Sphingosine was purchased from Focus Biomolecules (PA, USA). β -D-Galactopyranosyl-(1 \rightarrow 4)- β -D-glucopyranosyl-(1 \rightarrow 1')-D-erythro-sphingosine was purchased from Avanti Polar Lipids, Inc. (AL, USA). 4-(4,6-Dimethoxy-1,3,5-triazin-2-yl)-4-methylmorpholinium chloride (DMT-MM) was purchased from Tokyo Kasei Inc. (Tokyo, Japan). Fatty acid free BSA was purchased from Sigma-Aldrich Corp. (MO, USA).

High-performance thin layer chromatography silica gel 60 RP-18 F₂₅₄S (HPTLC) plates and silica gel were purchased from Merck Millipore (Darmstadt, Germany). Spectra/Por 7 dialysis tubing 12 mm [flat width] \times 90 mm [length], MWCO: 15,000 was purchased from Spectrum Chemical Mfg. Corp. (NJ, USA). TiO₂ was generously donated by Toho Titanium Co. Ltd. (Kanagawa, Japan). All solvents and reagents used were HPLC grade or LC-MS grade.

¹H NMR (500 MHz) spectra and other 2D experiments were performed on an AVANCE III 500 spectrometer (Bruker Biospin

GmbH, Bremen, Germany) in deuterated solvent using Me₄Si (0.00 ppm) as the internal standard. High-resolution mass spectra (HRMS) were recorded on AccuTOFLC-plus JMS-T100LP mass spectrometer coupled with ESI interface (JEOL Ltd.; Tokyo, Japan).

nano LC-FLD-ESI-MS set-up and conditions

Cell extracts were analysed using a Nano Frontier nLC digital nanoflow HPLC system (Hitachi High-Tech Corp., Tokyo, Japan). A tapered capillary column filled with C18 silica particles (particle size: 3 µm; 75 µm [i.d.] × 150 mm [length]; Nikkyo Technos Co., Ltd., Tokyo, Japan) was used as a sprayer tip. Mobile phase A was water and mobile phase B was acetonitrile. A step gradient condition was applied as the glycolipid mixture contained both acidic and neutral molecules. The mobile phase conditions were as follows: from 0 to 5 minutes, 5% B and 95% A; from 5 to 15 minutes, 95% B and 5% A; and from 15 minutes until the end of the run, 100% B. The pump was operated at a flow rate of 200 nL/min. The sample injection volume was 1 µL and the separation temperature was approximately 25 °C. Samples were dissolved in an ethanol:water (3:7) solution prior to injection. Fluorescence detection was carried out using an OptiTool FLE1100 Type B (Ikeda Scientific Co. Ltd., Tokyo, Japan) equipped with a fibre-optic cable and a collimator was used for irradiating excitation light (Ex., 470 nm) and acquiring emission light (Em., 520 nm). Data were collected at 0.20 s intervals using Smart Chrom software (KYA Technologies Co., Tokyo, Japan).

The MS conditions were as follows. Samples of extracted glycolipids from PC12D were analysed using a quadrupole ion trap mass spectrometer (QIT-MS) coupled with a nanoelectrospray interface (amaZon ETD; Bruker Daltonics GmbH, Bremen, Germany), which was attached to a three-dimensional manipulator for fluorescence detection. The parameters for analysis were (1) dry temperature, 120 °C; (2) dry gas (N₂), 4.0 L/min; (3) scan range, *m/z* 500–2000; (4) compound stability, 100%; (5) target mass, *m/z* 1000; (6) ion charge control (ICC), on, target, 200,000; (7) maximum accumulation time, 200 ms; (8) average, seven spectra; and (9) polarity, negative and positive. In our MS/MS experiments, the end-cap radio frequency amplitude was 1.2 V and the isolation width was *m/z* 4.0. This system set-up is similar to a previously reported set-up [8,10].

Cell imaging using laser scanning confocal microscopy

Cell imaging was performed using a FluoView FV1000-D laser scanning confocal microscope with an UPLSAPO water-immersion objective lens (60×, NA = 1.35; Olympus, Tokyo, Japan). Laser beams from diode lasers with a wavelength of 483 and 559 nm were used for the excitation of BODIPY FL C₅ and BODIPY TR fluorophores, respectively. The excitation laser beams were passed through a dichroic mirror (DM405/473/559) and the fluorescence emission was separated with beam splitters (SDM473 and SDM560) and then passed through a barrier filter (BA490-540 and BA575-675). The laser unit, confocal microscope, and detection units were connected to a computer and controlled using Olympus FluoView software (version 3.1a). A Nikon A1R equipped with a 37 °C temperature control stage and a Plan Apo VC water-

immersion objective lens (60×, NA = 1.20; Nikon, Tokyo, Japan) was also used for cell imaging. Laser beams from diode lasers with a wavelength of 488 nm were used for excitation of BODIPY FL C₅ and eGFP. The fluorescence emission was passed through a barrier filter (BA525-575). The laser unit, confocal microscope, and detection units were connected to a computer and controlled using NIS Elements AR (version 4.51.00)

Preparation of fluorescent lactosyl sphingosine and sphingosine analogues

Lactosyl sphingosine and sphingosine analogues were prepared according to our previous report with slight modifications [8-10].

Compound **1** was prepared by adding DMT-MM (3.4 mg, 12.3 µmol) to a solution consisting of β-D-Galactopyranosyl-(1→4)-β-D-glucopyranosyl-(1→1')-D-erythro-sphingosine (1.9 mg, 3.0 µmol) dissolved in 200 µL of tetrahydrofuran (THF):H₂O (3:1) and BODIPY FL C₅ (1.0 mg, 3.0 µmol) dissolved in 100 µL of THF:H₂O (3:1). The mixture was stirred for 2 h at 40 °C. The resulting mixture was subsequently purified by preparative thin layer chromatography (PTLC) (CHCl₃:MeOH:H₂O, 40:10:1). A band with *R_f* = 0.4 was collected and extracted with CHCl₃:MeOH (2:1) to yield **1** (72%). Product formation was confirmed using NMR (Fig. S1-S4) and ESI-HRMS in positive mode. The *m/z* of sodiated LacCerBODIPY (**1**), C₄₆H₇₄BF₂N₃NaO₁₃, was predicted to be 948.5175 and a peak was observed at 948.5303.

Compound **2** was prepared by adding β-D-Galactopyranosyl-(1→4)-β-D-glucopyranosyl-(1→1')-D-erythro-sphingosine (1 mg, 1.6 µmol) dissolved in 50 µL of THF:H₂O (3:1) to a solution of succinimidyl ester of BODIPY TR-X (1.25 mg, 1.97 µmol) dissolved in 100 µL THF:H₂O (3:1). The resulting mixture was stirred overnight at 37 °C and subsequently purified by silica gel chromatography (CHCl₃:MeOH:H₂O, 40:10:1). A band with *R_f* = 0.2 was collected and extracted with CH₂Cl₂:MeOH (2:1) to yield LacCerBODIPY TR-X (**2**). Product formation was confirmed by using NMR (Fig. S5 and S6) and ESI-HRMS in the positive mode. The *m/z* of compound **2**, C₅₇H₈₁BF₂N₄O₁₅SNa, was predicted to be 1165.5372 and a peak was observed at 1165.5861.

Compound **3** was prepared by adding DMT-MM (4.8 mg, 17.3 µmol) to a solution consisting of BODIPY FL C₅ (1.3 mg, 4.1 µmol) in 100 µL of THF:H₂O (3:1) and D-erythro-sphingosine (1.0 mg, 3.3 µmol) in 200 µL of THF:H₂O (3:1). The mixture was stirred overnight at 40 °C and subsequently purified by PTLC (CHCl₃:MeOH, 10:1). A band with *R_f* = 0.77 was collected and extracted with CHCl₃:MeOH (10:1) to yield **3**. Product formation was confirmed using NMR (Fig. S7 and S8) and ESI-HRMS in the positive mode. The *m/z* of compound **3**, C₃₄H₅₄BF₂N₃O₃Na, was predicted to be 624.4119 and a peak was observed at 624.4218.

Preparation of BSA complex of fluorescent analogues

A complex of fluorescent analogues with BSA was prepared according to the reported procedure [8-10]. For example, 2.9 µmol of LacCerBODIPY **1** was dried and then dissolved in 200 µL of ethanol and added dropwise to 4 mL of Dulbecco's phosphate-buffered saline (D-PBS) containing 193 mg (2.9 µmol) of BSA while being vortexed. The complex was dialysed overnight at 4 °C against 500 mL of D-PBS and then

ARTICLE

OBC

ultracentrifuged (100,000× g) at 4 °C for 20 minutes. The supernatant was collected and frozen at −20 °C in an Eppendorf tube for storage. Before use, the complex was diluted with the cell culture medium as required.

Expression of actin-binding protein LifeAct fused with yield enhanced GFP (LifeAct-eGFP)

The plasmid for the retrovirus vector expressing LifeAct-eGFP (pCX4 bsr/hygro LifeAct-eGFP) was prepared using a Retrovirus Packaging Kit Eco (TaKaRa Bio, Otsu, Japan) and used to transfect PC12D cells. Detailed information is provided in Supporting information (Table. S1).

Cell culture and uptake of fluorescent compounds

PC12D cells were grown in Dulbecco's Modified Eagle Medium (DMEM) supplemented with 1% (v/v) GlutaMAX-I, 10% (v/v) heat-inactivated horse serum, 5% (v/v) heat-inactivated calf serum, 1% (v/v) streptomycin, and penicillin at 37 °C with 5% CO₂. The medium was replaced every day. For cell imaging, 40% confluent cells on a 35 mm glass bottom dish coated with collagen (Cellmatrix Type IV; Nitta Gelatin Inc., Osaka, Japan) were used. For differentiation, 50 µg/mL NGF was added to the cells for a specific time, based on experimental needs.

Cells were incubated with 2.5 µM LacCerBODIPY (1)–BSA complex in DMEM for one minute (pulsed) at room temperature. Other compounds, LacCerBODIPY TR-X (2), CerBODIPY (3), and CerBODIPY TR (4) were introduced into cells in the same manner. After the cells were rinsed once in medium, they were incubated under the maintenance conditions described above until the cells were imaged. Cells measuring 40% confluency on a 100 mm dish were used for the analysis of cellular metabolites of fluorescently tagged molecules. The cells were incubated with 2.5 µM LacCerBODIPY (1)–BSA complex in medium for five minutes at 37 °C with 5% CO₂. After the cells were rinsed twice by saline, they were incubated under the maintenance conditions described above until cell collection.

Cell collection and lipid extraction

Cells were harvested by treatment with a trypsin–EDTA solution and collected in a tube and centrifuged to obtain pellets. The pellets were rinsed with saline and stored at −80 °C. The frozen stocks were defrosted, kept on ice, and then freeze–thawed with liquid nitrogen. Total lipids were extracted with 20-fold (w/v) chloroform:MeOH (1:2, v/v) under sonication for 30 min, and centrifuged to remove the supernatant, and further extracted with chloroform:MeOH (2:1, v/v) containing 5% (v/v) water under sonication for 30 min, and centrifuged. The combined supernatant was dried using a SpeedVac vacuum concentrator. The lipid extract was pre-treated with TiO₂ † [18] by mixing it with chloroform:MeOH (3:7, v/v) containing 0.1% (v/v) acetic acid and centrifuging to collect the supernatant. For the analysis, the extract was dissolved in 50 µL of ethanol:water (3:7), from which 1 µL (2% of the extract) was used.

FRAP analysis of glycolipids

PC12D cells were stained with 2.5 µM LacCerBODIPY (1)–BSA complex, 2.5 µM LacCerBODIPY TR (2)–BSA complex, 0.5 µM CerBODIPY (3)–BSA complex, or 0.5 µM CerBODIPY TR (4)–BSA

complex using a pulse-chase method. The FRAP experiment was performed using an Olympus FV1000-D confocal microscope system or a Nikon A1R confocal laser scanning microscope with a 60× water-immersion objective. The excitation laser wavelength was 488 nm for BODIPY FL C₅ and 559 nm for BODIPY TR. The radius of the desired circular region of interest (ROI: 3.0–3.9 µm) was selected on the cell membrane. The imaging size was 256 × 256 pixels and the scan speed was 2.0 µs per pixel. The experiments began by obtaining three images to record the prebleach intensity at 2.0% laser power, followed by full laser power photobleaching and a postbleach sequence of 37 images. Fluorescence intensity in the ROI was adjusted using background subtraction. The values from the analyses were calculated with nonlinear regression software, ORIGIN 8 (OriginLab, MA, USA), using the following equation:

$$y = I_0 + (I^\infty - I_0) \times \{x / (x + t_{50})\}$$

where y is the recovery ratio at the arbitrary point in time (x), I_0 is the intensity value immediately after bleaching, and I^∞ is a theoretical plateau value for the recovery ratio (the so-called mobile fraction). Here, t_{50} is the time required to achieve half the value of I^∞ , which depends on the average speed of the marker molecules in the ROI.

Results and discussion

Internalisation of LacCerBODIPY (1) in undifferentiated and differentiated PC12D cells

PC12D cells differentiate into neuron-like cells with an NGF treatment of 48–72 hours †† [15]. A previous investigation revealed that glycan structures of GSLs drastically change during cell differentiation [19]. However, time-resolved investigation has not been carried out, thus the details of glycan processing events remain unclear. We are interested in determining the

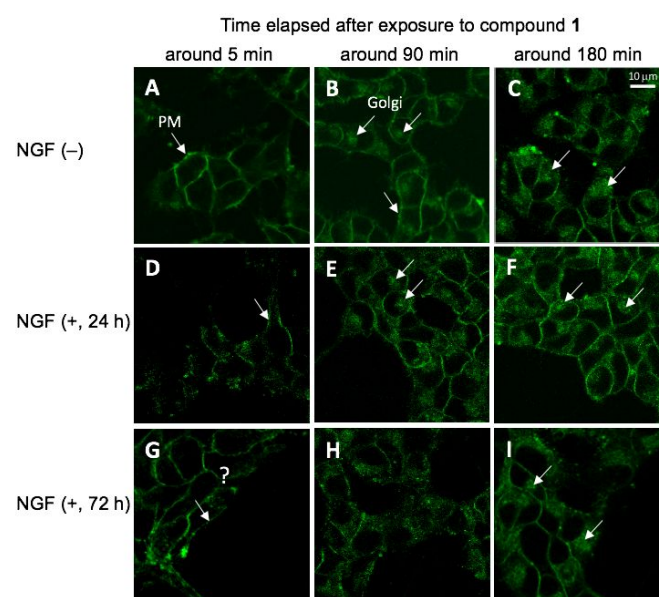


Fig. 2. Time study of the localisation of compound 1 in different culture conditions of PC12D cells; undifferentiated states (A, B, and C), differentiated states after 24 h NGF stimulation (D, E, and F), and differentiated states after 72 h NGF stimulation (G, H, and I).

cellular state associated with pathological changes that may be useful in understanding the events connected with glycan processing during the differentiation process. Thus, LacCerBODIPY (**1**) was pulse-introduced into cultured PC12D cells, in which localisation was visualised in a time-resolved manner. A one-minute pulse time was selected based on our previous results obtained from experiments on CHO-K1 cells [9].

We selected the following three distinctive cell states: undifferentiated cells not treated with NGF, cells treated with NGF for 24 hours, and cells treated with NGF for 72 hours. The cells were treated with compound **1** complexed with BSA as described in the previous studies [8,9]. In all cases, **1** was gradually internalised and would reappear on the membrane 90 minutes after it disappeared from the plasma membrane (Fig. 2). This recycling was somewhat unclear, as the cellular organelles were still stained when the fluorescence returned to the plasma membrane; a phenomenon that did not occur with CHO-K1 cells [9]. This might indicate that the internalisation process is slower, the Golgi is less active in PC12D cells, or both. The complexity of glycan structures in PC12D cells may also play a role, as CHO-K1 cells are known to produce GM3 ganglioside, single sialic acid is α -linked to 3-position of galactose, only from lactosyl ceramide [20-22].

The fluorescence on the plasma membrane remained for more than ten minutes after one-minute pulse introduction of **1** in differentiated cells. The delay of the internalisation process may indicate that plasma membrane-based lipid recycling is markedly slow. Fluorescence on the plasma membrane slowly disappeared after 30 minutes and was almost gone within 90 minutes (Fig. S9). At this time, the fluorescence reappeared on the plasma membrane and the organelles were still stained.

Time-resolved glycan transformation using compound **1**

It has been reported that the composition of glycan structures in undifferentiated and differentiated PC12D cells is

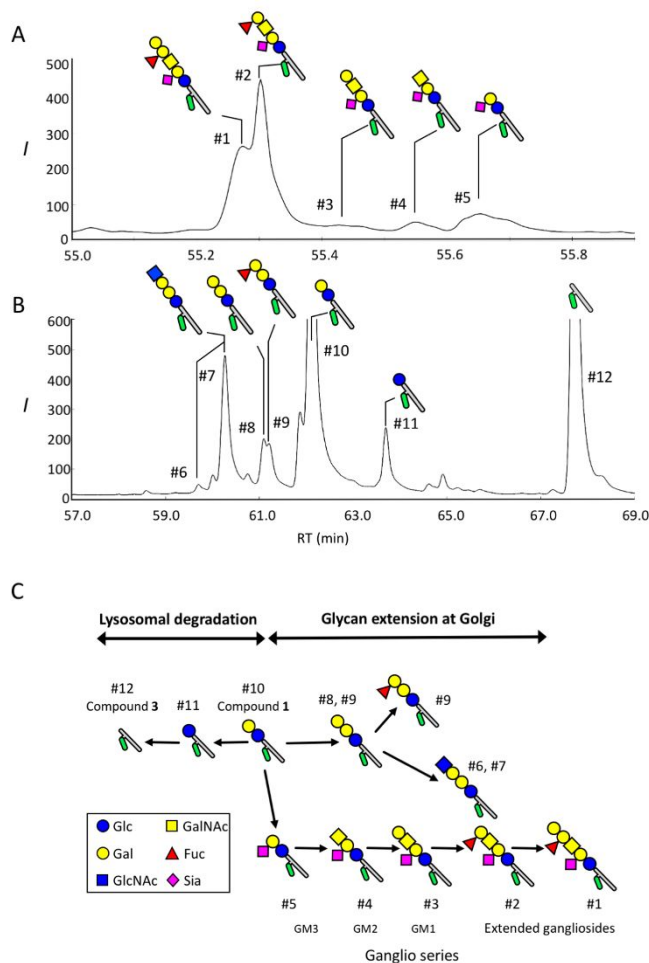


Fig. 3. Nano LC analysis of fluorescent components in undifferentiated PC12D cells. Typical nano LC-FLD chromatograms of gangliosides (A) and neutral glycolipids peaks (B). Peaks 6 and 7 had same m/z value and were considered to be stereo- or linkage-isomers. C. Plausible synthetic scheme estimated by the sequence information obtained by MS.

Representative drawings of the glycan structure symbols followed the "Symbol Nomenclature for glycans" guidelines by the NCBI (<https://www.ncbi.nlm.nih.gov/glycans/snfg.html>).

quite different and an increase of unusual neutral Globo GSLs after treatment with NGF has been observed [19,23]. The importance of information regarding glycan profiles is recognised as the glycan profile is known to reflect cellular differential stages that relate to differentiation lineage, genetic subtypes, and evolutionary lineages. However, there has to be a point in time when a cell changes to a specific glycoform.

We decided to analyse glycan processing using LacCerBODIPY (**1**) in a time-resolved manner. Compound **1** complexed with BSA was introduced into three culture set-ups and the fluorescent molecules were extracted and analysed using nano LC-FLD-ESI-MS. Since our analysis set-up is capable of detecting fluorescence, the glycan transformation can be quantitatively analysed. A typical fluorescence detected nano LC chromatogram is shown in Fig. 3A and 3B, where both glycan synthesis and degradation were observed. A series of ganglio-type and other glycans with CerBODIPY that lost Gal and Glc can be seen. It is noted that some of the glycans at retention times of approximately 55.3 and 61.0 minutes were fucosylated. From these analyses, we could estimate a plausible glycan transformation pathway taking continuity of individual ion species as shown in Fig. 3C.

In order to compare the glycan profiles of cells with undifferentiated, differentiated, and transitioning states, three

culture conditions of NGF(-), NGF(+) with 72 hours incubation, and NGF(+) with 3 hours incubation were investigated. Detailed analyses of the results obtained over time were carried out (Table 1).

Previous reports often discuss the structures and functions of gangliosides after anion exchange resin purification. In our experiments, a TiO₂-column was used to remove a large amount of endogenous phospholipids which disrupt LC analysis[‡]. All the BODIPY-carrying molecules, except for the sphingomyelin analogue, were extracted and subjected to nano LC-FLD-ESI-MS analysis. Based on the MS analysis, both *N*-acetyl and *N*-glycoryl sialic acid-containing species were observed and were combined to obtain the area in LC.

It was shown that certain GSLs were synthesised specifically depending on the differentiation state (Fig. 4 and Table 1). Suppression of glycan synthesis was observed in the well differentiated cells after 72 hours of incubation compared with the other experiments. The consumption rate of compound **1** showed that approximately 60% was transformed into either higher GSLs or degraded into Cer derivative **3** in NGF(-) (Table 1A) and NGF(+) under differentiation (Table 1B); however the conversion rate slowed down to about 40% in the differentiated state (Table 1C). In all cases, it was observed that degradation was the main process compared with the glycosylation processes for this particular compound (**1**), which might be a limitation. More importantly, the conversion of **1** appeared to reach a quasi plateau, indicating that the BODIPY-carrying ceramide derivative **3** is accepted by PC12D cells and is recycled as a mimetic of ceramide. The time to reach equilibrium was comparable to that reported in experiments using 6-[*N*-(7-nitro-2,1,3-benzoxadiazol-4-yl)amino]hexanoyl (NBD)-tagged ceramide [24].

Table 1. Composition^o of the fluorescent molecules (%) in PC12D cells as obtained by nanoLC-FLD-MS

peak #	Structure ^b	A. NGF(-); Compound 1 only was added												B. NGF and compound 1 were added at the same time												C. Cells were exposed to compound 1 after treatment with NGF for 72 hr.											
		Observed <i>m/z</i> values ^c				[M+H] ⁺ ^e				Incubation time (h)				Incubation time (h)				Incubation time (h)				Incubation time (h)															
		1	3	6	9	1	3	6	9	1	3	6	9	1	3	6	9	1	3	6	9	1	3	6	9	1	3	6	9								
1	Hex(Fuc)HexHexNAc(Sia5Ac)(Gc)GalGlc-R	1889.3	1905.3	0.08	0.14	0.52	0.89	1.80	2.06	0.06	0.18	0.37	0.42	1.03	1.35	0.00	0.00	0.00	0.00	0.00	0.00	0.00	0.00	0.00	0.00	0.00	0.00	0.23	0.53								
2	FucHexHexNAc(Sia5Ac)(Gc)GalGlc-R	1727.2	1743.2	0.06	0.20	0.31	0.52	0.99	0.89	0.07	0.19	0.53	0.77	1.46	1.53	0.00	0.00	0.00	0.00	0.00	0.00	0.00	0.00	0.00	0.00	0.00	0.10	0.34	0.47								
3	HexHexNAc(Sia5Ac)(Gc)GalGlc-R	1581.1	1597.1	0.00	0.00	0.00	0.06	0.14	0.17	0.03	0.05	0.10	0.13	0.19	0.13	0.00	0.00	0.00	0.00	0.00	0.00	0.00	0.00	0.00	0.00	0.00	0.10	0.16	0.16								
4	HexNAc(Sia5Ac)(Gc)GalGlc-R	1419.1	1435.1	0.00	0.00	0.00	0.10	0.20	0.24	0.05	0.03	0.10	0.15	0.31	0.24	0.00	0.00	0.00	0.00	0.00	0.00	0.00	0.00	0.00	0.00	0.00	0.14	0.15	0.15								
5	Sia5Ac(Gc)GalGlc-R	1216.0	1232.0	0.10	0.28	0.49	0.66	0.69	0.56	0.18	0.53	1.14	0.99	1.06	0.72	0.12	0.00	0.00	0.00	0.00	0.00	0.00	0.00	0.00	0.00	0.30	0.48	0.41									
6	HexNAcHexGalGlc-R	1151.7	-	0.57	0.86	0.70	0.55	0.62	0.74	0.06	0.56	0.64	0.64	0.52	0.55	0.56	0.48	1.11	0.44	0.33	0.61	0.61	0.61	0.61	0.61	0.61	0.61	0.61	0.61								
7	HexNAcHexGalGlc-R	1151.7	-	1.32	2.55	2.97	4.91	6.34	10.62	1.13	2.71	3.91	5.18	7.10	9.97	1.74	1.28	3.03	1.92	2.79	5.65	5.65	5.65	5.65	5.65	5.65	5.65	5.65	5.65								
8	HexGalGlc-R	1110.7	-	0.75	0.90	1.68	1.70	3.58	2.62	0.30	0.76	1.25	1.27	1.54	1.63	0.71	0.48	0.43	0.44	0.56	1.12	1.12	1.12	1.12	1.12	1.12	1.12	1.12	1.12								
9	HexGalGlc-R / FucHexGalGlc-R	1110.7	1256.6	-	0.79	1.41	1.56	2.37	3.56	5.07	1.28	1.53	2.37	2.86	3.83	5.46	0.90	0.73	1.54	1.45	1.49	3.25	3.25	3.25	3.25	3.25	3.25	3.25	3.25								
10	GalGlc-R (1)	948.7	-	91.18	77.51	65.71	51.77	43.29	42.28	92.12	82.81	62.50	53.52	47.44	41.47	84.41	82.88	78.04	77.76	75.53	63.39	63.39	63.39	63.39	63.39	63.39	63.39	63.39	63.39								
11	Glc-R	786.6	-	1.13	9.38	15.84	24.28	24.14	17.92	0.51	0.73	3.15	3.07	4.15	4.73	6.59	8.00	6.60	8.23	5.29	9.24	9.24	9.24	9.24	9.24	9.24	9.24	9.24	9.24								
12	R (Spingosine-BODIPY, 3)	624.5	-	2.21	3.94	7.37	9.82	12.06	13.23	1.76	5.71	9.77	13.76	15.51	19.64	3.20	3.81	4.81	6.89	10.46	12.29	12.29	12.29	12.29	12.29	12.29	12.29	12.29	12.29								
	sum of unknown compounds	1.81	2.83	2.84	2.37	2.61	3.80	2.46	3.80	2.46	4.22	14.18	17.25	15.89	12.60	1.76	2.34	4.44	2.57	2.26	2.72	2.72	2.72	2.72	2.72	2.72	2.72	2.72	2.72								

^o Composition of individual molecules were determined based on the area obtained by fluorescence detector for nanoLC.^b Hex: hexose, HexNAc: *N*-acetyl hexosamine, Sia: sialic acid^c Positive and negative ions were detected in MS by switching the polarity.^d Neutral molecules were observed as sodiated ions in MS.^e Acidic molecules carrying Sia were observed as deprotonated ions in MS.

ARTICLE

OBC

When we focused on ganglioside synthesis, fucosylated

Hex(Fuc)HexHexNAc(Neu5Ac/Gc)GalGlcCerBODIPY was found to be a major component (ca 2%) and the ratio of Hex(Fuc)HexHexNAc(Neu5Ac/Gc)GalGlcCerBODIPY and FucHexHexNAc(Neu5Ac/Gc)GalGlcCerBODIPY was about 3:1 in undifferentiated PC12D cells (Fig. 4). The former ganglioside has been reported as a malignancy associated marker and the latter was confirmed during rat development [25-27]. The synthesis of these gangliosides was diminished to about 1% in differentiated cells (Fig. 4B). The ratio of these gangliosides was about 1:1 and the conversion rate remained the same as in the differentiated state when we analysed the conversions immediately after treating the cells with NGF (under differentiation). It should be noted that the initial speed of GM3 synthesis was higher than other GSLs. Although GM3 remained one of the major gangliosides in undifferentiated state as well as during differentiation, the amounts of GM1 and GM2 were very small, suggesting that these are transiently formed intermediates in both states (Fig. 4A and 4C). The fucosylation of several GSLs was observed. Our analysis results do not entirely agree with the reported steady state glycan distribution that may relate to a different fatty acyl moiety. However, it was shown that compound **1** can be used to distinguish cell states.

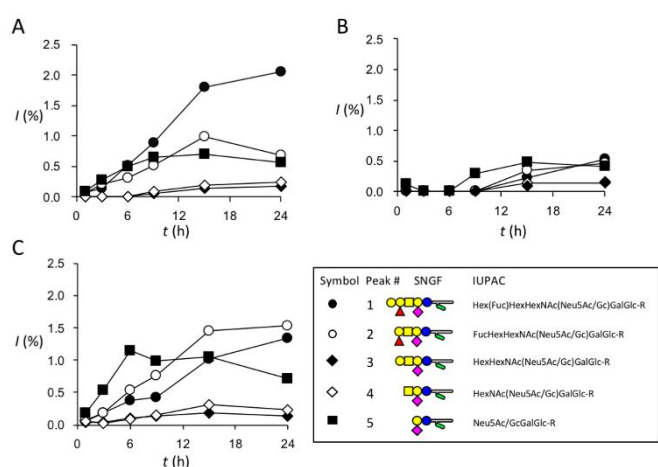
FRAP analysis of compound **1** on plasma membrane

Fig. 4. The proceeding gangliosides were quantified in different culture conditions of PC12D cells at an undifferentiated state (A), differentiated state (B), and during differentiation (C).

FRAP is often used to investigate membrane fluidity by using green fluorescent protein (GFP)-fused membrane proteins [28]. The fact that compound **1** remained on the plasma membrane for approximately 10 minutes (Fig. S9) prompted us to examine FRAP to determine the membrane fluidity change in response to an NGF treatment. Since some of the GSLs including LacCer are known to exist in a raft, the mobility of such GSLs may be slower than other membrane lipids. Lipid rafts consist of GSLs, cholesterol, and distinctive proteins that are often associated with cellular skeletal structure; the fluorescently tagged compound may reflect the cellular state.

The cultured PC12D cells were analysed by FRAP with and without exposure to NGF. In the case of NGF treatment, one-minute pulse was used. The focus area (region of interest; ROI) was set to a diameter of 3.9 μm . After the fluorescence at a focus area is bleached, nearby molecules diffuse into the ROI and the fluorescence recovers depending on the physical properties of the molecule. Although the ROI is often selected at a flat surface of the plasma membrane at the top or bottom of adhesive cells, we chose an ROI at the periphery of the cell at a confocal point. Additionally, we selected a slight offset from the cell to avoid the effects of nearby cellular organelles, such as endosomes and lysosomes, and also to create a vertical ellipse area at the plasma membrane that is similar to the horizontal ROI area (Fig. 5A).

As seen in Fig. 5B, where the fluorescence recovery was plotted over time, the fastest recovery rate was observed immediately after NGF stimulation. A slower recovery rate indicates that a portion of the fluorescent compound **1** is trapped in a membrane fraction with slow mobility, such as raft [29]. The response time resembled the lamellipodia formation that is related to Rho family GTPases in response to NGF treatment [30,31].

We further investigated the effect of NGF treatment on membrane dynamics in detail. In this experiment, the fluorescence recovery yield (I^∞ ; intensity reach to a plateau) and t_{50} value (time required for the intensity to reach to half the value of I^∞) used to estimate the diffusion velocity were obtained at 24 and 72 hours after NGF treatment with a one minute pulse of compound **1** prior to the FRAP experiments.

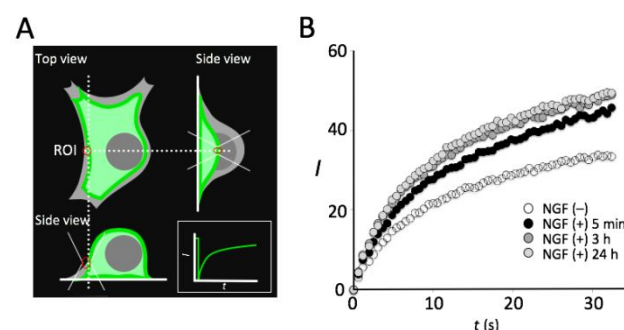


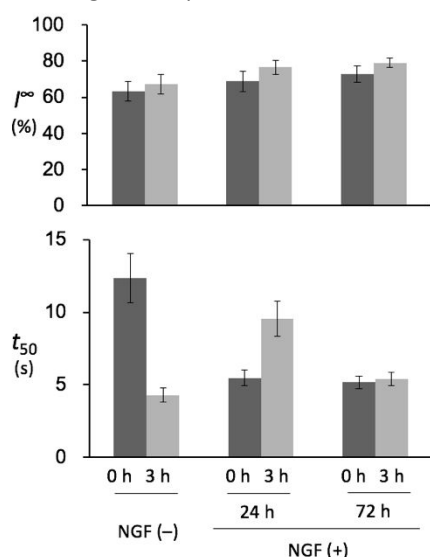
Fig. 5. Selecting an ROI on the plasma membrane (A) and time study of membrane fluidity changes as visualised by fluorescence recovery after NGF stimulation (B).

NGF was also removed when compound **1** was pulsed to avoid any complexity. The ROI was set to a diameter of 3.0 μm .

Our experimental set-up consisted of a group with NGF stimulus that was divided into two subgroups with an incubation time of 24 or 72 hours after stimuli and a group without NGF stimulus (Fig. 6). I^∞ for non-treated group, stimulated for 24, and 72 hours immediately after pulse introduction (0 hour) of **1** were $63.3 \pm 5.5\%$, $68.8 \pm 5.4\%$, and $72.8 \pm 4.7\%$, respectively. I^∞ for the same set of experiments after 3 hours, when fluorescence reappeared in plasma membrane, were $67.2 \pm 5.3\%$, $76.6 \pm 3.8\%$, and $79.0 \pm 2.5\%$, respectively. Although the difference is small, the same tendency was observed in the case where a slightly larger ROI was used.

The t_{50} value changes were more dramatic; t_{50} values for non-treated, stimulated for 24, and 72 hours immediately after pulse introduction of **1** were 12.3 ± 1.7 , 5.5 ± 0.5 , and 5.2 ± 0.4 seconds, respectively, and 4.3 ± 0.5 , 9.5 ± 1.2 , and 5.4 ± 0.4 seconds, respectively for 3 hours after introduction of **1**. The t_{50} values immediately after the compound pulse showed that NGF treated cells have smaller apparent t_{50} values. This might be explained by the different internalisation speed of **1** relying on lipid recycling and the density difference between **1** and the membrane. Since the concentration of a molecule affects the diffusion speed, the t_{50} value of **1** on the plasma membrane should reflect its membrane density. If the NGF untreated cells have a faster lipid recycling rate (Fig. S9), the density of **1** in undifferentiated cells is smaller than NGF treated cells, and thus the apparent rate of diffusion in differentiated cells may be faster with a smaller t_{50} value.

The t_{50} values obtained after 3 hours of compound introduction were markedly different from that of 0 hour. In this series of experiments, the t_{50} value obtained for 24 hour-NGF treatment was higher compared to that obtained with the other



treatments. Three hours after the introduction of **1**, a portion of

Fig. 6. The fluorescence recovery yields (I^∞) and t_{50} values obtained by FRAP analysis just after introduction and 3 h after introduction of compound **1** into different states of cells: undifferentiated state (A), differentiated state after 24 h NGF stimulation (B), and differentiated state after 72 h NGF stimulation (C). $n=7$

1 was converted into various GSLs as shown in the above section, although the amount was small. We first considered that the presence of a certain GSL caused a change in the diffusion rate, but this is unlikely considering the transformation rate. Therefore, the reformation of cytoskeletal structure that occurs during cell development, which drives the distinguishable physical properties of the plasma membrane, must be related to some component of cellular dynamics other than glycan structure. This will be discussed in the next section.

FRAP analysis comparison of LacCerBODIPY with LifeAct-eGFP

To ascertain the relationship between changes in plasma membrane dynamics and the cytoskeleton, we focused on a type of actin that relates to nerve-like extension. In PC12D cells, Rac signalling triggers actin fibre reformation [32] leading to ruffling after NGF treatment and before nerve-like extension [33,34]. We focused on the movement of F-actin and expression of the actin-binding protein LifeAct of which the N-terminal α -helix fused with yield enhanced GFP (LifeAct-eGFP) [35-38].

Fluorescence on the plasma membrane was bleached in a ROI (3.0 μm in diameter) and the fluorescence recovery was monitored for a set of experiments with and without NGF stimulus. The I^∞ and t_{50} values of LifeAct-eGFP for NGF treated cells where FRAP was carried out after five minutes of NGF stimulus were $46.5 \pm 5.7\%$ and 3.4 \pm 1.0 seconds, and those for NGF(-)-cells were $50.5 \pm 7.2\%$ and 4.7 \pm 1.6 seconds, respectively (Fig. 7). The respective I^∞ and t_{50} values of LacCerBODIPY **1** were $40.4 \pm 4.8\%$ and 2.5 \pm 0.6 seconds, and 49.0 \pm 6.1% and 1.9 \pm 0.5 seconds, respectively. There was not much difference in I^∞ , but the t_{50} values of both **1** and LifeAct were reduced in response to the NGF stimulus. We concluded that LacCerBODIPY (**1**) is useful for examining plasma membrane fluidity and that the fluidity change occurs immediately after NGF treatment, which is associated with actin reformation.

Effect of fluorescent tag in LacCerBODIPY (**1**)

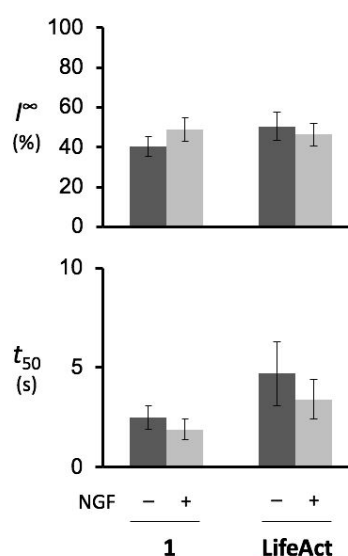
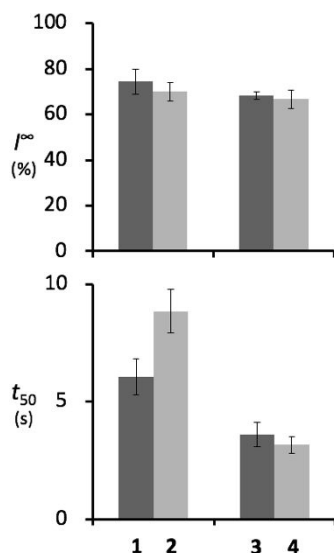


Fig. 7. The fluorescence recovery yields (I^∞) and t_{50} values obtained by FRAP analysis using compound **1** and LifeAct-eGFP. $n=7$



We examined the possible effects of the fluorescent reporter group, as the BODIPY tag that replaced the fatty acyl

Fig. 8. The effects of the fluorescent tag on the chemical properties of probe molecules **1**, **2**, **3**, and **4**. $n=7$

group in the ceramide structure might cause changes in physical properties. In order to investigate the effect of the fluorescent tag and glycan on the physical properties of compound **1**, we decided to use a series of compounds **1**, **2**, **3**, and **4** (Fig. 8). For the selection of fluorophores besides their excitation-emission wavelength, we considered calculated Log P values that is important in partition between water and lipid membrane. The individual CLog P values are 2.72 (**1**), 3.43 (**2**), 6.57 (**3**), and 7.51 (**4**). We considered that the tag should be kept in the lipid structure as a reporter group since the relatively hydrophobic fluorescent tag in the hydrophilic carbohydrate changes the overall properties drastically. After several considerations, we made a series of compounds: **2**, **3**, and **4**. In these compounds, we examined the effect of green BODIPY C5 in **1** in the presence of the glycan portion while a slight change in BODIPY dye is made. The focus areas were set to a diameter of 3.9 μm in these experiments.

The effect of glycan was greater than that of the fluorophore as the t_{50} values of Cer derivatives (**3** and **4**) were faster than those of the LacCer derivatives (**1** and **2**) in both fluorophores (Fig. 8). The larger t_{50} value of **2** with BODIPY TR-X indicates that the internalisation of **2** is slower than **1**, which supports our previous hypothesis that the internalisation of the compound **1** reflects its density in the plasma membrane, lowering the t_{50} values. The slower rate of internalisation of **2** has also been previously reported [10].

The estimated diffusion rates of LacCer analogues **1** and **2** are in the range of the rates for membrane proteins [39] with about 10% glycerolipid concentration. It is conceivable that the compounds with a lactose portion enter the lipid raft on the plasma membrane, which also agrees with the previous result of F-actin mobility.

Conclusion

Glycolipid transformation for three distinct differentiation states in cultured PC12D cells was successfully tracked by analysing LacCerBODIPY, a fluorescently labelled compound. The analysis was carried out by utilising our previously reported analysis platform, in-column fluorescence detected nanoLC-ESI-MS, that allowed for simultaneous quantitative and qualitative analysis. It was found that suppression of glycan synthesis was observed in the differentiated state. LacCerBODIPY was also used to observe membrane fluidity based on FRAP experiments, which led us to find differences in plasma membrane fluidity occurring immediately after NGF stimulation (about 5 minutes) before neuron-like outgrowth starts. These results suggest that LacCerBODIPY can be used, not only in the analysis of glycolipid metabolism, but also in distinguishing between different cellular states. This method could be an alternative method to evaluate cell states, such as the malignant transformation of a cancer cell at an early stage, which does not depend on a specific marker molecule.

Conflicts of interest

There are no conflicts to declare.

Acknowledgements

This work was supported in part by ERATO from the Japan Science and Technology Agency (JST). The authors thank to Dr. Koichi Miura (Kyusyu University) for generously providing the plasmid for the retrovirus vector expressing LifeAct-eGFP (pCX4 bsr/hygro LifeAct-eGFP).

Notes and references

- ‡ It was also found that ZrO_2 cartridge column can be used instead of TiO_2 . [7]
- ‡‡ Time course study of nerve-like projection extension on NGF treatment after 48 hours was also carried out, of which result is provided in supporting information (Fig. S10).
- 1 Y. Shinohara, N. Fujitani, and J. Furukawa, *Trends Glycosci. Glycotech.* 2013, **25**, 103–116.
 - 2 B.L. Stocker and M.S.M. Timmer, *ChemBioChem* 2013, **14**, 1164–1184.
 - 3 Y. Xia and L. Peng, *Chem. Rev.* 2013, **113**, 7880–7929.
 - 4 S. Chatterjee, K.S. Clarke, and P.O. Kwitrovich Jr, *J. Biol. Chem.* 1986, **261**, 13480–13686.
 - 5 C.S. Chen, G. Bach, and R.E. Pagano, *Proc. Natl. Acad. Sci. U. S. A.* 1998, **95**, 6373–6378.
 - 6 V. Puri, R. Watanabe, R.D. Singh, M. Dominguez, J.C. Brown, C.L. Wheatley, D.L. Marks, and R.E. Pagano, *J. Cell Biol.* 2001, **154**, 535–547.
 - 7 O.C. Martin and R.E. Pagano, *J. Cell. Biol.* 1994, **125**, 769–781.
 - 8 A. Ohtake, S. Daikoku, K. Suzuki, Y. Ito, and O. Kanie, *Anal. Chem.* 2013, **85**, 8475–8482.
 - 9 Y. Kanie, M. Taniuchi, and O. Kanie, *J. Chromatogr. A* 2018, **1534**, 123–129.
 - 10 S.-H. Son, S. Daikoku, A. Ohtake, K. Suzuki, K. Kabayama, Y. Ito, and O. Kanie, *Chem. Commun.* 2014, **50**, 3010–3013.
 - 11 S. Daikoku, Y. Ono, A. Ohtake, Y. Hasegawa, E. Fukusaki, K. Suzuki, Y. Ito, S. Goto, and O. Kanie, *Analyst*, 2011, **136**, 1046–1050.

- 12 N. Komura, K.G. Suzuki, H. Ando, M. Konishi, M. Koikeda, A. Imamura, R. Chadda, T.K. Fujiwara, H. Tsuboi, R. Sheng, W. Cho, K. Furukawa, K. Furukawa, Y. Yamauchi, H. Ishida, A. Kusumi, and M. Kiso, *Nat. Chem. Biol.* 2016, **12**, 402–410.
- 13 R. Katoh-Semba, S. Kitajima, Y. Yamazaki, and M. Sano, *J. Neurosci. Res.* 1987, **17**, 36–44.
- 14 H. Nagase, T. Yamakuni, K. Matsuzaki, Y. Maruyama, J. Kasahara, Y. Hinohara, S. Kondo, Y. Mimaki, Y. Sashida, A.W. Tank, K. Fukunaga, and Y. Ohizumi, *Biochemistry* 2005, **44**, 13683–13691.
- 15 K. Fujita, P. Lazarovic, and G. Guroff, *Environ. Health Perspect.* 1989, **80**, 127–142.
- 16 M. Sano and M. Iwanaga, *Cell Struct. Funct.* 1992, **17**, 341–350.
- 17 M. Takefuji, K. Mori, Y. Morita, N. Arimura, T. Nishimura, M. Nakayama, M. Hoshino, A. Iwamatsu, T. Murohara, K. Kaibuchi, and M. Amano, *Biochem. Biophys. Res. Commun.* 2007, **355**, 788–794.
- 18 Y. Ikeguchi and H. Nakamura, *Anal. Sci.* 2000, **16**, 541–543.
- 19 T. Ariga and R. K. Yu, *Neurochemical Research* 1998, **23**, 291–303.
- 20 E.B. Briles, E. Li, and S. Kornfeld, *J. Biol. Chem.* 1977, **252**, 1107–1116.
- 21 V.M. Rosales Fritz, J.L. Daniotti, and H.J.F. Maccioni, *Biochem. Biophys. Acta* 1997, **1354**, 153–158.
- 22 S. Uemura, S. Yoshida, F. Shishido, and J.-I. Inokuchi, *Mol. Biol. Cell* 2009, **20**, 3088–3100.
- 23 T. Kanda, T. Ariga, M. Yamawaki, S. Pal, R. Katoh-Semba, and R.K. Yu, *J. Neurochem.* 1995, **64**, 810–817.
- 24 T. Babia, J. W. Kok, C. Hulstaert, H.de Weerd, and D. Hoekstra, *Int. J. Cancer* 1993, **54**, 839–846.
- 25 E. H. Holmes and S.-I. Hakomori, *J. Biol. Chem.* 1982, **257**, 7698–7703.
- 26 A. Suzuki, I. Ishizuka, and T. Yamakawa, *J. Biochem.* 1975, **78**, 947–954.
- 27 J.F. Bouhours, and G.C. Hansson, *J. Biol. Chem.* 1987, **262**, 16370–16375.
- 28 E.A.J. Reits and J.J. Neefjes, *Nature Cell Biol.* 2001, **3**, E145–E147.
- 29 A.K. Kenworthy, B.J. Nichols, C.L. Remmert, G.M. Hendrix, M. Kumar, J. Zimmerberg, and J. Lippincott-Schwartz, *J. Cell Biol.* 2004, **165**, 735–746.
- 30 K. Aoki, T. Nakamura, and M. Matsuda, *J. Biol. Chem.* 2004, **279**, 713–719.
- 31 I. de Curtis and J. Meldolesi, *J. Cell Sci.* 2012, **125**, 4435–4444.
- 32 R.A. Gungabissoon and J.R. Bamburg, *J. Histochem. Cytochem.* 2003, **51**, 411–420.
- 33 M. Sano, M. Iwanaga, H. Fujisawa, M. Nagahama, and Y. Yamazaki, *Brain Res.* 1994, **639**, 115–124.
- 34 E. Jin, K. Nosaka, and M. Sano, *Neurochem. Int.* 2007, **51**, 216–226.
- 35 A. Lopata, R. Hughes, C. Tiede, S.M. Heissler, J. R. Sellers, P.J. Knight, D. Tomlinson, and M. Peckham, *Sci. Rep.* 2018, **8**, 1–15.
- 36 J. Riedl, A.H. Crevenna, K. Kessenbrock, J.H. Yu, D. Neukirchen, M. Bista, F. Bradke, D. Jenne, T.A. Holak, Z. Werb, M. Sixt, and R. Wedlich-Soldner, *Nat. Methods* 2008, **5**, 605–607.
- 37 J. Riedl, K.C. Flynn, A. Raducanu, F. Gärtner, G. Beck, M. Bösl, F. Bradke, S. Massberg, A. Aszodi, M. Sixt, and R. Wedlich-Söldner, *Nat. Methods* 2010, **7**, 168–169.
- 38 N. Nakai, K. Sato, T. Tani, K. Saito, F. Sato, and S. Terada, *Microscopy*, 2019, **68**, 359–368.
- 39 A. Nenninger, G. Mastroianni, A. Robson, T. Lenn, Q. Xue, M.C. Leake, and C.W. Mullineaux, *Mol. Microbiol.* 2014, **92**, 1142–1153.